Econ. Environ. Geol.
Vol. 27, No. 5, p. 499-505, 1994.

Analysis of Micro- to Macro-Mechanics in Granitic Rock : Experimental Observation and Theoretical Consideration

Gyo-Cheol Jeong*

ABSTRACT : Local stress concentrations often cause new micro-damaging induced by a healed pre-existing defects, and the macro-damage is developed by propagation and coalescence of the micro-damage. The micro-damage causes non-linear deformation in rock material. Considerable work has also been applied to describe mathematically the behavior of cracks under stress. Although these mathematical models can usually be made to agree quite well with the measured data, but it is questionable how well the models describe real rock including microcracks in pre-failure state, such as their micro-damage mechanisms. In the present study, micro-damage initiation and propagation in granitic rock under increasing stress were observed directly. Furthermore, a stress analysis considering the bisphere model was carried out using the homogenization theory to analyze the mechanics of the stress-induced micro-damage.

INTRODUCTION

Micro-damaging process determines their macroscopic mechanical response. Granite commonly involves complex composite microcrack systems which are caused by different geologic processes and under varying conditions (Kranz, 1983).

Microcrack studies are of increasing interest in geophysics and civil engineering related to underground space development and radioactive waste disposal. Theoretical works relating microcrack density and microcrack geometry to material modulus reduction (Walsh, 1965; O'Connel et al., 1974) and recent studies relating crack density to material strength reduction (Horii et al., 1986; Ashby et al., 1986, 1990) have suggested that it would be possible to obtain a complete and testable theory of macro-damage in rocks. However, numerical analysis of stress distribution around micro-damage, that is, microcracking at grain contact due to deformation of the specimen, have not been studied sufficiently up to the present.

Microscopic studies of cracks in postloaded samples have been made using scanning electron microscopy (SEM) in order to reveal interactions between microcracks and relationships between the concentrated microcracks and macroscopic failure (Friedman et al., 1978; Wong, 1982; Mardon et al., 1990). These experimental studies have shown that macroscopic fractures grow from microcracks, which are abundantly found in crystalline rocks. However, these works have a drawback; they have been performed only under zero stress conditions using thin or cut section after experiment, or under artificially fractured conditions.

To better understand the fundamental problems of micro-damage occurrence and propagation at the grain contact area within granite, I have observed the actual microcrack behavior during the deformation of granite specimens. Experimental studies of microcrack initiation at the grain contact portion of coarse-grained granite were carried out under uniaxial compressive stress using a newly developed experimental system (Jeong and Ichikawa, 1994). This experimental system enables a continuous observation of microcracking under loading. In addition, since visible stress-induced microcracks during loading cannot be visualized in the unloading state in conventional experimental method, direct observation under loading is very important for an accurate understanding of true micro-damage. Furthermore, the homogenization theory (Sanchez-Palencia, 1980)) was used to analyze the stress concentration in the vicinity of the microcracks at grain contact and variation of elastic modulus during microcracking. Opening of healed pre-existing microcracks parallel to applied stress often caused new microcracking, and simultaneously these new microcracking are affected by the elastic mismatch of two grains such as quartz and feldspar. Details of experiments were given by Jeong and Ichikawa (1994).

PRE-EXISTING MICROCRACKS

Pre-existing microcracks within originally intact rocks are very important in causing initial micro-damage in rocks. Before specimens are loaded, many healed pre-

*Korea Institute of Geology, Mining and Materials, Taejon 305-350, Korea

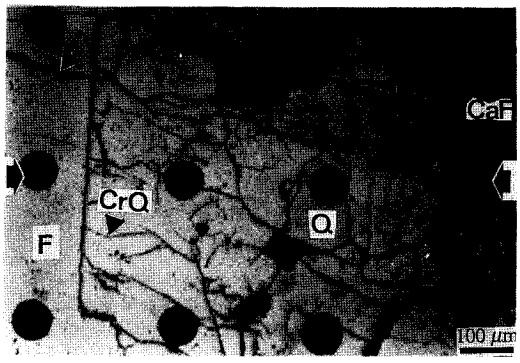

Fig. 1. Photomicrograph showing stress-induced micro-damaging at quartz (Q)-feldspar (F) contact portion. Large solid circles were marked for confirmation of observation area.

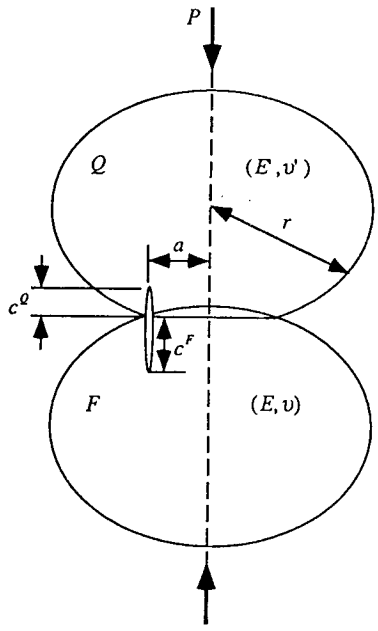

Fig. 2. Hertzian loading arrangement showing a schematic array of a grain contact.

existing microcracks (indicated by CrQ in Fig. 1) can be observed in quartz grains, and some longish microcavities (indicated by CaF in Fig. 1) with blunt ends are observed in feldspar.

Jeong et al. (1993, 1994) described these long rows of microcavities as healed microcracks with almost completely leaked fluid inclusion. They observed that microcracks were preferentially developed in quartz of granite, and most of them were intracrystalline, frequently starting at grain boundaries. Therefore, these microcracks can be visualised as pre-existing intracrystalline microcracks, and their systems may be considered as microcracks caused by internal stress due to change of pressure and/or temperature.

MICRO-DAMAGE INITIATION AND PROPAGATION

The primary intracrystalline microcracks, that is, the cleavage and coincident boundary microcracks in feldspar grains, are initiated through the defective cleavage (CaF in Fig. 1) and the grain boundary at a stress level 30 *MPa*. At the same time, microcavities are linked, and intracrystalline microcracks and grain boundary microcracks parallel or subparallel to the axial stress direction are predominantly caused by tensile stress due to the Poisson effect in nature. Furthermore, local variations in elastic properties of different minerals or the presence of microcracks cause the stress to be concentrated, and the remote compressive stresses are converted to locally tensile stresses. Based on these facts, intracrystalline microcracks nearly parallel to the axial stress direction are initiated from pre-existing grain boundary microcracks between quartz and feldspar grain.

ANALYSIS

Estimation of micro-damage initiation and propagation

Since most of grains are in contact with each other, we base our interpretation for microcrack initiation and propagation at contact portion of grains on the special nature of the stress field of Hertzian loading (Wilshaw, 1971). The radius a, as shown in Fig. 2, of the circle of contact between spherical two grains are formed from the Hertzian analysis:

$$a^3=\frac{3}{4}Pr\left[\frac{(1-\upsilon^2)}{E}+\frac{(1-\upsilon'^2)}{E'}\right] \quad (1)$$

where P is the normal load applied on the grain, E' and E are the Young's moduli of quartz and feldspar grains, respectively, and υ' and υ are the corresponding values of the Poisson ratio.

The primary stress-induced intracrystalline microcrack is initiated from contact portion of two grains. While the crack is small and normal to the contact surface, the maximum tensile stress σ_m^Q and σ_m^F in the quartz and feldspar grains are uniformly distributed along the microcrack and the microcracking criterion is assumed equivalent to that for a single edge microcrack in tension (Wilshaw, 1971). The stress intensity factors K_I^Q and K_I^F, which are function of the stress and the microcrack

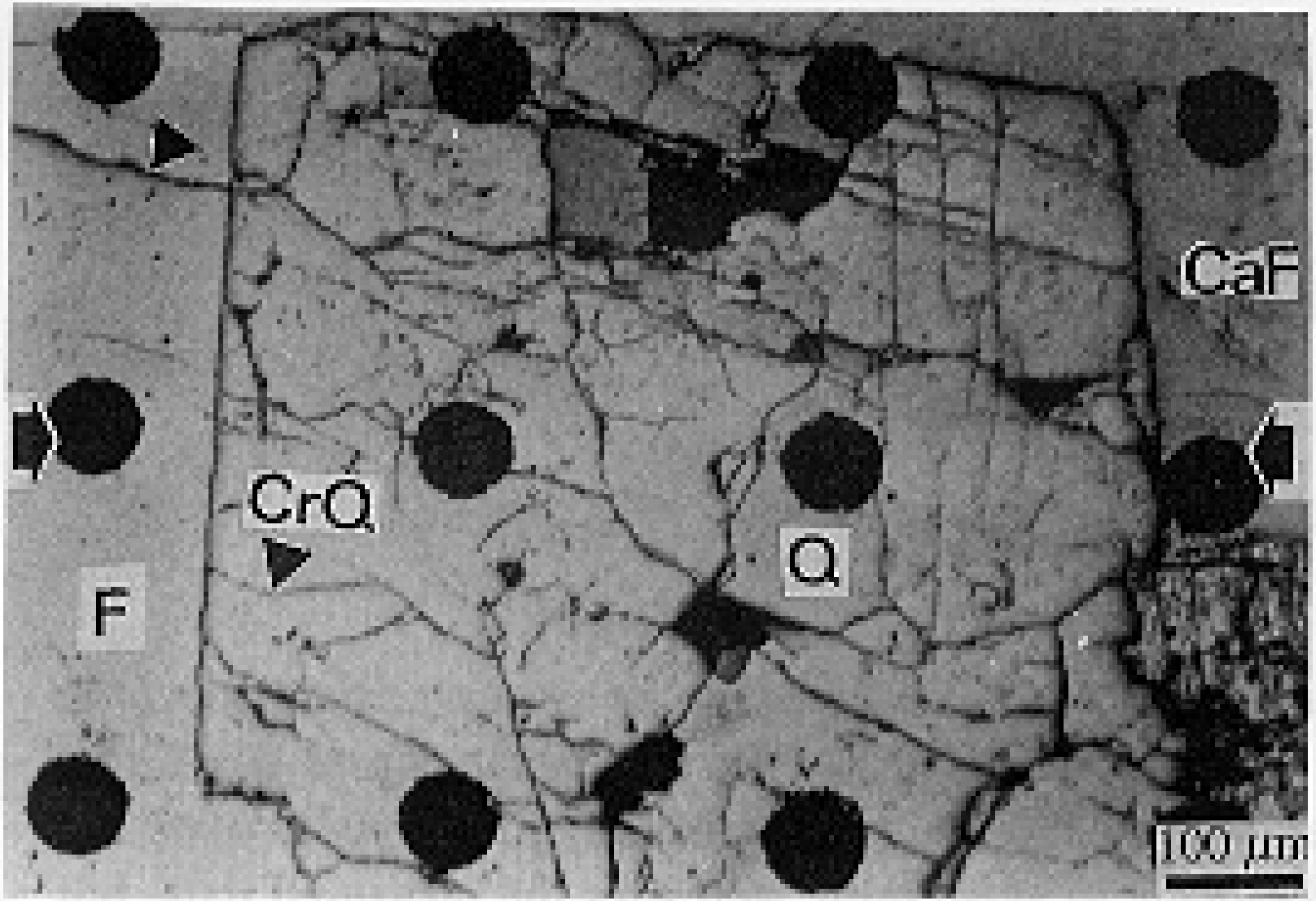

Fig. 1. Photomicrograph showing stress-induced micro-damaging at quartz (Q)-feldspar (F) contact portion. Large solid circles were marked for confirmation of observation area.

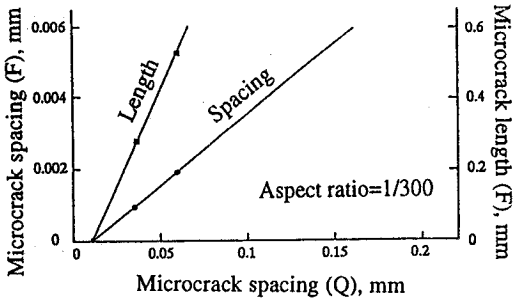

Fig. 3. Graphs showing relation between microcrack spacing and length in feldspar (F) and microcrack spacing in quartz (Q).

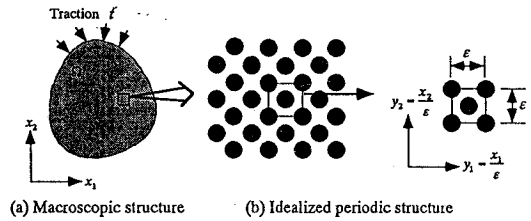

Fig. 4. Macroscopic and microscopic periodic structure.

length c^Q and c^F are given by

$$K_I^Q = 1.12\sigma_m^Q(\pi c^Q)^{1/2} \tag{2}$$

$$K_I^F = 1.12\sigma_m^F(\pi c^F)^{1/2} \tag{3}$$

where

$$\sigma_m^Q = \frac{(1-2\upsilon')P^Q}{2\pi a^2} \tag{4}$$

$$\sigma_m^F = \frac{(1-2\upsilon)P^F}{2\pi a^2} \tag{5}$$

By substituting equation (4) and (5) into equation (2) and (3), we obtain the critical forces for the initiation of microcracks in quartz and feldspar grain as

$$P^Q_{critical} = \frac{2\pi a^2 K_{IC}^Q}{1.12(\pi c^Q)^{1/2}(1-2\upsilon')} \tag{6}$$

$$P^F_{critical} = \frac{2\pi a^2 K_{IC}^F}{1.12(\pi c^F)^{1/2}(1-2\upsilon)} \tag{7}$$

In this case, we should assume that the local stress field in the vicinity of the microcrack is solely due to the elastic contact between two grains (Zhang et al., 1990). This is a reasonable assumption in our microcrack initiation analysis since the contact stress concentration is highly localized and the microcrack length at the initiation of Hertzian fracture is very short (Zhang et al., 1990).

We now evaluate the characteristics for microcrack growth. Since at a contact portion of two grains, $P^Q_{critical}$ must be equal to $P^F_{critical}$, we obtain the following relation :

$$\frac{K_{IC}^F}{K_{IC}^Q} = \frac{(1-2\upsilon)}{(1-2\upsilon')} \cdot \left(\frac{c^F}{c^Q}\right)^{1/2}$$

where the critical stress intensity factors of quartz and feldspar have been measured by Atkinson et al. (1980) for several orientation. We take their average critical stress intensity factors $0.383\,MPa\sqrt{m}$ for K_{IC}^Q and $0.364\,MPa\sqrt{m}$ for K_{IC}^F. The Poisson ratios are obtained as $\upsilon' = 0.109$ and $\upsilon = 0.299$ by Birch (1961). By using these values, we obtain the microcrack growth condition as :

$$c^F = 3.42c^Q \tag{9}$$

However, if open pre-existing intracrystalline microcracks are developed in quartz and feldspar grains, the Hertzian theory presented here is not applicable.

In bisphere model, relation between the microcrack spacing and length in feldspar and microcrack spacing in quartz for input data of computation is shown in Fig. 3.

Homogenization Theory for Elastic Problem

The homogenization theory allows us to derive microscopic stress distributions which account for the micro-damage initiation of rocks. This theory can be applied when the media being investigated have a periodic structure (Sanchez-Palencia, 1980). Macroscopic equivalent structure is called the homogenized structure and its behavior coefficients are the homogenized coefficients. Furthermore, by a localization procedure, the theory allows an easy computation of the microscopic field of stresses and, in particular, of stress forces at the boundaries between two grains. These overstresses, at the microscopic level, can initiate microcracks.

Consider a composite material formed by the spatial repetition of a unit cell made of different material as shown Fig. 4. Let us assume that a body characterized by the domain Ω, for example, made of two different materials whose mixture is represented by a unit cell that is very small, of order ε compared with the dimensions of the structural body Ω. We denote that the elasticity tensor is $E^\varepsilon(x)$, body force is $f^\varepsilon(x)$, the traction is t, and the displacement is $u^\varepsilon(x)$. Then static equilibrium using weak form on the body can be stated as

$$\int_\Omega E_{ijkl}^\varepsilon(x) \frac{\partial u_k^\varepsilon(x)}{\partial x_l} \frac{\partial v_i^\varepsilon(x)}{\partial x_j} dx \tag{10}$$

$$=\int_{\Omega} f_i^{\varepsilon}(x)v_i^{\varepsilon}(x)dx+\int_{\partial\Omega} t_i(x)v_i^{\varepsilon}(x)dx$$

where, $v(x)$ is arbitrary admissible displacement, and superscript ε is used to indicate dependence on the microstructure.

If the body is subjected to some load and boundary conditions, the resulting deformation and stresses, in general, rapidly vary from point to point because of repetition of microscopic unit cells, it may be considered that all quantities have two explicit dependencies. One is on the macroscopic level x, and the other is on the microscopic level x/ε. In order to introduce a function depending on the microscopic level, we may take the microscopic variable $y=x/\varepsilon$. Accordingly, $\varepsilon^{\varepsilon}(x)$ $f^{\varepsilon}(x)$, and $u^{\varepsilon}(x)$ have the two variable functions as follows:

$$\begin{aligned} E^{\varepsilon}_{ijkl}(x)&=E_{ijkl}(x,\frac{x}{\varepsilon})=E_{ijkl}(x,y)\\ f^{\varepsilon}_i(x)&=f_i(x,\frac{x}{\varepsilon})=f_i(x,y)\\ u^{\varepsilon}_i(x)&=u_i(x,\frac{x}{\varepsilon})=u_i(x,y)\end{aligned} \tag{11}$$

These functions are, in general, Y-periodic functions on $y\in Y$. Differentiation of two variable function is given by following operator such as

$$\frac{\partial}{\partial x_j}\rightarrow\frac{\partial}{\partial x_j}+\frac{1}{\varepsilon}\frac{\partial}{\partial y_j} \tag{12}$$

The solution $u^{\varepsilon}(x)$ from boundary conditions of the function (10) makes it reasonable to assume that $u^{\varepsilon}(x)$ can be expressed as an asymptotic expansion of the displacement field in the form:

$$u^{\varepsilon}(x)=u(x,y)=u^0(x)+\varepsilon u^1(x,y)+\varepsilon^2u^2(x,y)+\cdots;\ y=\frac{x}{\varepsilon} \tag{13}$$

and

$$v^{\varepsilon}(x)=v(x,y)=v^0(x)+\varepsilon v^1(x,y)+\varepsilon^2v^2(x,y)+\cdots \tag{14}$$

where, $u^1, u^2\cdots$ are Y-periodic function with respect to the variable $y\in Y$. The first term u^0 of the expansion of u^{ε} in ε does not depend on the microscopic variable y but depends only on the macroscopic scale x. In other words, u^0 represents, essentially, the macroscopic mechanical behavior while the u^1, $u^2\cdots$ represent the microscopic behavior.

Introducing equations (11), (12), (13) and (14) into equation (10), and solving the limit $\varepsilon\rightarrow 0$, we can obtain equations on u^1 and u^2 (Sanchez-Palencia, 1980). First of all, the solution u^1 expresing the effect of microstructures can be written as follows:

$$u^1_i(x,y)=-\chi^{kl}_i(x,y)\frac{\partial u^0_k(x)}{\partial x_l}+\tilde{u}^1_i(x) \tag{15}$$

where, $\tilde{u}^1_i(x)$ is an arbitrary additive constant in y, that is, an integral constant on y. χ^{kl} is symmetric with respect to the indices k and l. This implies that six different vector functions are solved for the three-dimensional problem. Accordingly, the function is given by

$$\begin{aligned}&\int_Y E_{ijpq}(x,y)\frac{\partial\chi^{kl}_p(x,y)}{\partial y_q}\frac{\partial v_i}{\partial y_j}dy \\ &=\int_Y\Big(-\frac{\partial E_{ijkl}(x,y)}{\partial y_j}\Big)v_i dy=\int_Y E_{ijkl}(x,y)\frac{\partial v_i}{\partial y_j}dy\end{aligned} \tag{16}$$

Next, the solution u^0 can be written following global equilibrium equation for the macroscopic structure as:

$$\begin{aligned}&\int_{\Omega} E^H_{ijkl}(x)\frac{\partial u^0_k(x)}{\partial x_l}\frac{\partial v_i(x)}{\partial x_j}dx \\ &=\int_{\Omega}\tilde{f}_i(x)v_i(x)dx+\int_{\partial\Omega} t_i(x)v_i(x)dx\end{aligned} \tag{17}$$

where, homogenized elasticity tensor

$$E^H_{ijkl}(x)=\frac{1}{|Y|}\int_Y\Big(E_{ijkl}(x,y)-E_{ijpq}(x,y)\frac{\partial\chi^{kl}_p(x,y)}{\partial y_q}\Big)dy \tag{18}$$

where, $|Y|$ stands for the volume of the unit cell, and homogenized body force

$$\tilde{f}(x)=\frac{1}{|Y|}\int_y f_i(x,y)dy \tag{19}$$

are defined. Here, χ^{kl}, as shown in equation (16), is a vector function determined by the spatial repetition of microstructure consisting of microscopic unit cell, that is, this function is what is called a characteristic deformation function. Equation (15) shows that the displacement u^1 due to the microstructures is given by a form of multiplied average behavior strain $\partial u^0_k/\partial x_l$ multified by characteristic deformation function χ^{kl}. Comparing equation (17) with the original equation (10), we can find that if we use the elasticity tensor (18) and the body force (19) instead of $E^H_{ijkl}(x)$ and $\tilde{f}(x)$ respectively, then we can evaluate the average behavior u^0 of the material with microstructure. Equation (18) is also an integral on microscopic unit cell, and $E^H_{ijkl}(x)$ and $\tilde{f}_i(x)$, as average behavior, are equivalent to homogenized elasticity tensor and homogenized body force, respectively.

The stress in each point is given by constitutive equation as follows:

$$\sigma^{\varepsilon}_{ij}=E^{\varepsilon}_{ijkl}\frac{\partial u^{\varepsilon}_k(x)}{\partial x_l}\equiv\sigma^0_{ij}(x,y)+\varepsilon\sigma^1_{ij}(x,y)+\cdots \tag{20}$$

where, introducing $u^{\varepsilon}=u^0+\varepsilon u^1$ into equation (20), σ_{ij}, the approximation of the localized stress in microscopic unit cell, is given by

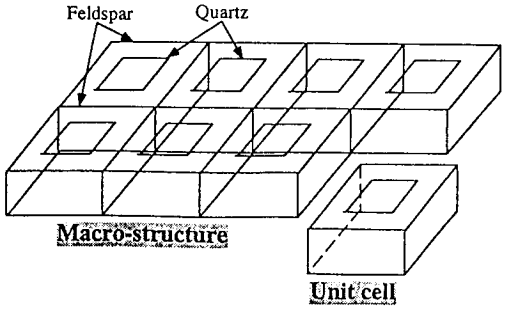

Fig. 5. Periodic model consisting of bisphere condition.

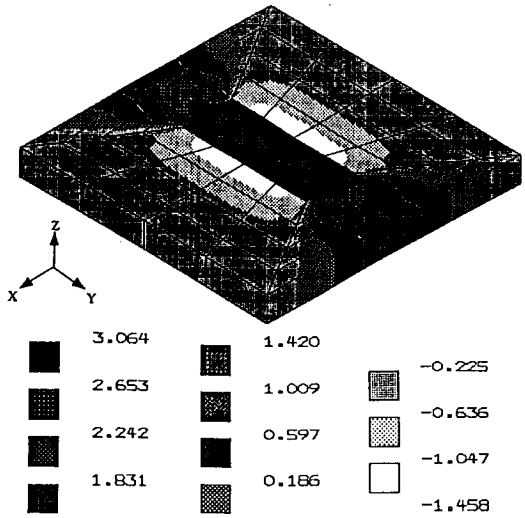

Fig. 6. Calculated contour map view of the normalized tensile stress in the contact portion of quartz-feldspar.

$$\sigma_{ij}(x,y)=\left(E_{ijkl}(x,y)-E_{ijpq}(x,y)\frac{\partial\chi_p^{kl}(x,y)}{\partial y_q}\right)\frac{\partial u_k^0(x)}{\partial x_l} \tag{21}$$

This localized stress $\sigma_{ij}(x,y)$ shows the stress field in microscopic unit cell, and the volume average in the unit cell is given by

$$\tilde{\sigma}_{ij}(x)=\frac{1}{|Y|}\int_Y \sigma_{ij}^0(x,y)dy \tag{22}$$

then equation (22) satisfies equilibrium equation as follows :

$$\int_\Omega \tilde{\sigma}_{ij}\frac{\partial v_i}{\partial x_j}dx=\int_\Omega f_i v dx \tag{23}$$

As shown above, from using homogenization theory, the average physical properties of the body, including microscopic repeated unit cell, can be computed, and localized stress distribution in arbitrary portion can be also estimated.

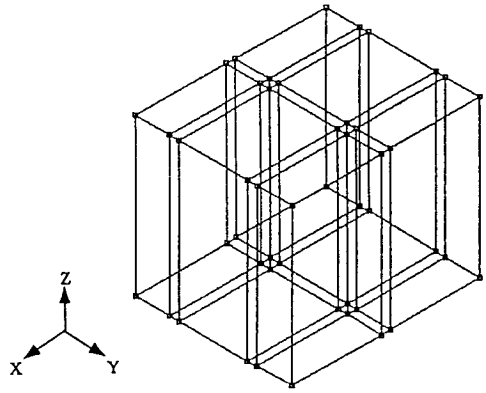

Fig. 7. Unit cell mesh for mechanical properties of quartz including healed pre-existing microcracks.

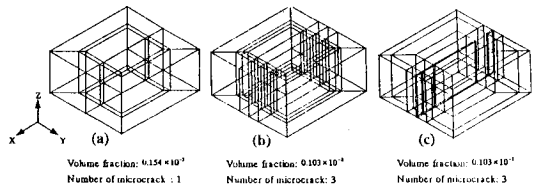

Fig. 8. Unit cell mesh for the microcrack propagation in bisphere model.

RESULTS

The granite used in the study may be considered in periodic material consisting of bisphere condition of quartz and feldspar (Fig. 5). First of all, for the first stage in the deformation, stress analysis in state in which pre-existing microcracks in quartz grain of unit cell were not initiated was carried out. Local values of the tensile stress normalized to the loading stress in the vicinity of the grain contact portion are shown in Fig. 6. The elastic coefficients of the quartz and feldspar have been measured by Birch (1961) etc., then we took the Young's modulus 87.5 GPa, Poisson's ratio 0.109 for quartz and average Young's modulus of orthoclase and plagioclase 67.6 GPa, Poisson's ratio 0.299 for feldspar.

Mechanical properties of quartz including healed pre-existing microcracks must be computed to determine those of quartz-feldspar system. Fig. 7 is mesh of unit cell in quartz grain including healed pre-existing microcracks. Variation of Young's modulus of quartz grain with opening of healed pre-existing microcracks is nonlinear.

Fig. 9 illustrates decreasing of normalized Young's modulus with increasing of volume fraction of stress-induced micro-damage in feldspar and anisotropy com-

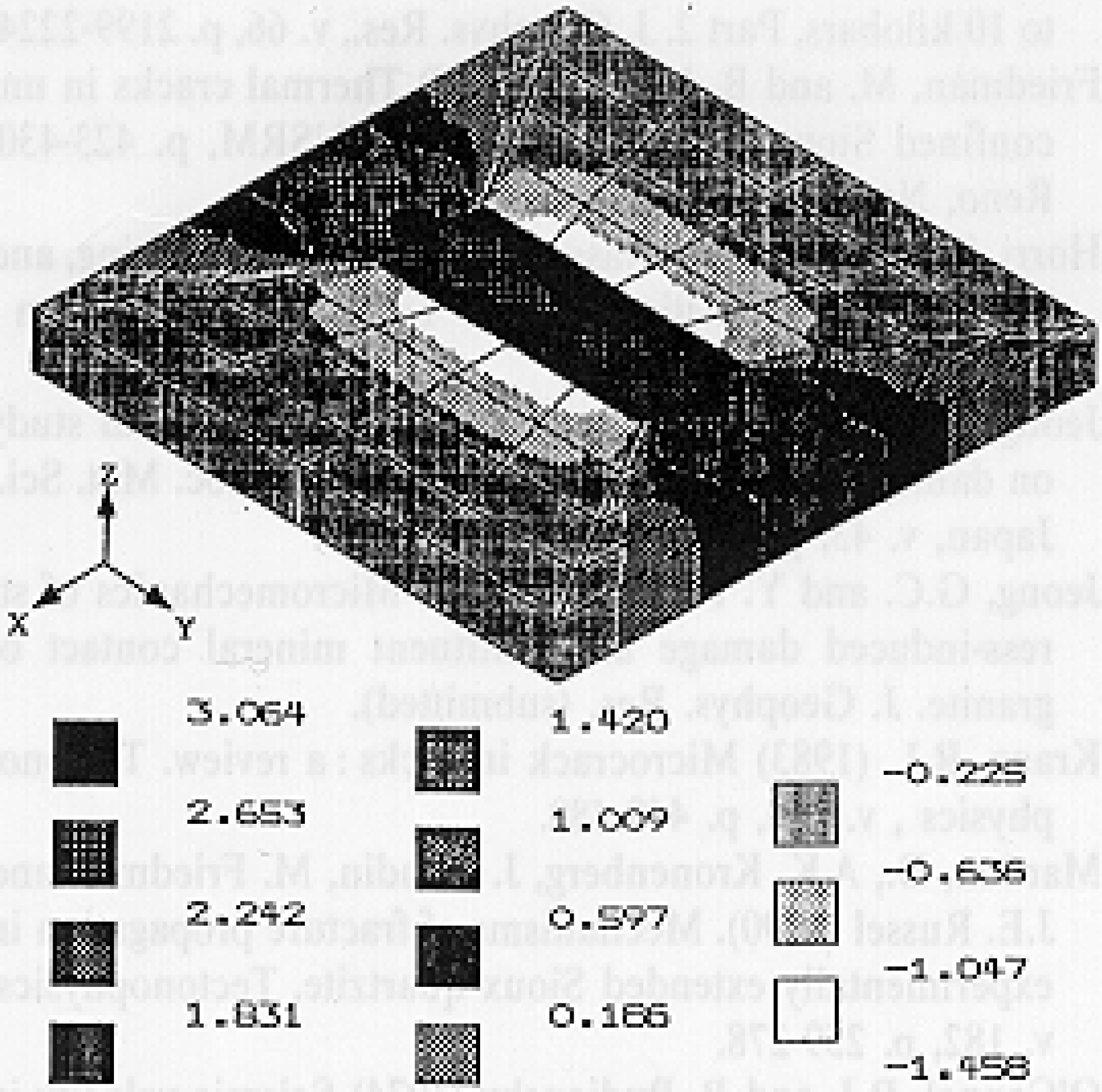

Fig. 6. Calculated contour map view of the normalized tensile stress in the contact portion of quartz-feldspar.

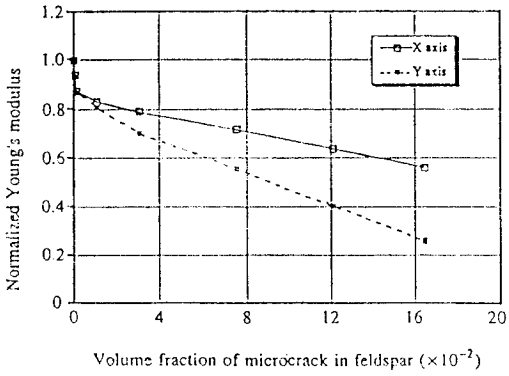

Fig. 9. Graphs showing decrease in normalized Young's modulus with increase in volume fraction of microcrack in feldspar.

puted from micro-damage propagation of Fig. 8, which is nonlinear that normalized Young's modulus drops fast as soon as stress-induced micro-damage initiate.

CONCLUSIONS

The aim of this paper is to provide some basis for a micromechanics of stress-induced damage occurring at the major constituent mineral contact portion of the granite. Micro-damaging in the contact of constituent minerals plays an important role in the nonlinear deformation process and leads to shear fracture of brittle material such as the granite under room temperature.

Granitic rocks, except biotite granite, also may be described in simplified terms as a two component system consisting of bisphere condition of quartz and feldspar.

Though the present study was limited only to the interaction of two minerals such as quartz and feldspar grain, most of granitic rocks also include micas and/or hornblende etc. and mechanical properties of the rock are more or less affected by them, which means that analysis for polycomponent system is necessary in multiple-grain interaction. However these problems may be reconsidered. Nevertheless, the present study is subjected to the basis of understanding the polycomponent system in polycrystalline rocks.

Finally, the important point of this study is that the analysis gives some idea of how micro-damaging can be triggered from a pre-existing microcrack.

REFERENCES

Ashby, M.F. and C.G. Sammis (1990) The damage mechanics of brittle solids in compression. Pure Appl. Geophys., v. 133, p. 489-521.

Ashby, M.F. and S.D. Hallam (1986) The failure of brittle solids containing small cracks under compressive stress states. Acta metall., v. 34, p. 497-510.

Atkinson, B.K. and V. Avdis (1980) Fracture mechanics parameters of same rock-forming minerals determined using an indentation technique. Int. J. Rock Mech. Min. Sci. Geomech. Abstr., v. 17, p. 383-386.

Birch, F. (1961) The velocity of compressional waves in rocks to 10 kilobars, Part 2. J. Geophys. Res., v. 66, p. 2199-2224.

Friedman, M. and B. Johnson (1978) Thermal cracks in unconfined Sioux quartzite. Proc. 19th USRM, p. 423-430. Reno, Nev.: Balkema.

Horri, M. and S. Nemat-Nasser (1986) Splitting, faulting, and brittle-ductile transition. Philos. Trans. R. Soc. London , v. 319, p. 337-374.

Jeong, G.C. and Y. Ichikawa (1994) An experimental study on damage propagation of intact granite. J. Soc. Mat. Sci., Japan, v. 43, p. 317-323 (in Japanese).

Jeong, G.C. and Y. Ichikawa (1993). Micromechanics of stress-induced damage at constituent mineral contact of granite. J. Geophys. Res. (submitted).

Kranz, R.L. (1983) Microcrack in rocks: a review. Tectonophysics , v. 100, p. 449-480.

Mardon, D., A.K. Kronenberg, J. Handin, M. Friedman and J.E. Russel (1990). Mechanisms of fracture propagation in experimentally extended Sioux quartzite. Tectonophysics, v. 182, p. 259-278.

O'Connel, R.J. and B. Budiansky (1974) Seismic velocity in dry and saturated cracked solids. J. Geophys. Res., v. 79, p. 5412-5426.

Sanchez-Palencia, E. (1980) Non-homogeneous media and vibration theory. Paris: Springer-Verlag. 480p.

Walsh, J.B. (1965) The effect of cracks on the uniaxial elastic compression of rocks. J. Geophys. Res. , v. 70, p. 399-411.

Wilshaw, T.R. (1971) The Hertzian fracture test. J. Phys. D., v. 4, p. 1567-1581.

Wong, T.F. (1982) Micromechanics of faulting in Wesrterly granite. Int. J. Rock Mech. Min. Sci., v. 19, p. 49-64.

Zhang, J., T.F. Wong and D.M. Davis (1990) Micromechanics of pressure-induced grain crushing in porous rocks. J. Geophys. Res., v. 95, p. 341-352.

Manuscript received 3, March 1994

화강암질암에 대한 미시적에서 거시적 손상역학의 해석 : 실험 및 이론

정 교 철

요 약 : 기존 미소결함에서의 국소적 응력집중은 새로운 미시적 손상의 원인이 되고, 이러한 미시적 손상은 또한 거시적 손상으로 발달하게 된다. 이들 미시적 손상에서 거시적 손상으로의 바달은 그 암석 및 암반의 변형특성으로 나타난다. 지금까지 응력하에서의 미소크랙의 거동에 대한 연구는 많이 되어왔으나, 실제암석의 파괴전 상태에서 미소크랙거동에 대한 역학적 해석은 아직 미비한 실정이다. 본 연구에서는 새로이 개발한 시험장치에 의한 정밀한 관찰로 손상 발달에 대한 이해를 더하였으며, 수학적 균질화 이론에 의해 수치해석함으로서 그 역학성을 검토하였다.